scientific reports

Check for updates

OPEN

Respiratory rate and minute ventilation independently modulate cardiovascular and autonomic responses in healthy adults

Haeyoung Choi[1,7], Chaeyeon Kim[1,7], Seokbeen Lim[3], Paul H. Min[3,4], Jeyeon Lee[5] & Dong Pyo Jang[2,6]✉

Respiration influences autonomic and cardiovascular function, yet the independent contributions of respiratory rate (RR) and minute ventilation (MV) remain unclear. We investigated how RR and MV independently and interactively affect cardiovascular and autonomic responses using a 2 × 2 controlled-breathing design in 19 healthy adults (24.6 ± 1.2 years): spontaneous RR versus slow RR (6 breaths/min), combined with MV at 100% versus 180% of resting baseline. We recorded heart rate (HR), stroke volume (SV), cardiac output (CO), and heart rate variability (SDNN). Elevating MV to 180% significantly increased HR (5–8%) and CO (6–12%) across both respiratory rates ($p < 0.01$), whereas changing RR alone at constant MV produced no significant cardiovascular effects. Temporal analysis revealed a mechanistically biphasic CO response: the early rise (minutes 1–2) was driven by increasing SV while HR remained stable, whereas the sustained later elevation was driven by progressive HR increases as SV declined. Slow RR increased HRV by 75–86% ($p < 0.01$), indicating increased overall heart rate variability, which may reflect enhanced autonomic flexibility. Notably, combining slow RR with high MV produced concurrent increases in both HR and HRV, diverging from the typical inverse HR-HRV relationship and suggesting sympathetic–parasympathetic co-activation. These findings demonstrate a clear bifurcation in cardiorespiratory control, identifying minute ventilation as the primary driver of short-term systemic cardiovascular modulation. In contrast, respiratory rate remains the dominant determinant of cardiac autonomic regulation (HRV).

Keywords Autonomic nervous system, Cardiac output, Heart rate, Heart rate variability, Minute ventilation, Respiratory rate

The modulation of respiration has long been recognized as a powerful tool for influencing autonomic and cardiovascular function[1]. Slow and controlled breathing practices, commonly used in meditation, yoga, and biofeedback, have consistently been shown to enhance vagal activity, reduce heart rate (HR), and improve baroreflex sensitivity[2,3]. Reducing the respiratory rate (RR) to approximately 6 breaths/min has been demonstrated to increase heart rate variability (HRV) and to decrease HR, reflecting enhanced parasympathetic modulation and autonomic balance[4,5].

While the effects of RR have been widely studied, the role of minute ventilation (MV), defined as the product of RR and tidal volume (TV), remains less well characterized. CO_2, acting through peripheral and central chemoreceptors, is the primary determinant/of ventilatory drive and regulates respiratory rhythm and metabolic gas exchange[6,7]. Functionally, MV determines the rate of CO_2 elimination and O_2 delivery, and it can distinctively modulate cardiovascular function through changes in intrathoracic pressure and venous return[8].

[1]Department of Electronic Engineering, Hanyang University, Seoul, Republic of Korea. [2]Department of Biomedical Engineering, Hanyang University, Seoul, Republic of Korea. [3]Department of Radiology, Mayo Clinic, Rochester, MN, USA. [4]Department of Physiology and Biomedical Engineering, Mayo Clinic, Rochester, MN, USA. [5]Department of Biomedical Engineering, College of Medicine, Hanyang University, Seoul, Republic of Korea. [6]Hypertix Inc., Seoul, Republic of Korea. [7]Haeyoung Choi and Chaeyeon Kim contributed equally to this work. ✉email: dongpjang@hanyang.ac.kr

For instance, an increase in TV, and consequently MV, can augment venous return and cardiac preload via the respiratory pump mechanism, potentially elevating stroke volume (SV) and cardiac output (CO)[6]. Conversely, while it has been proposed that excessive ventilation may trigger sympathetic cardiovascular responses[7], direct recordings of muscle sympathetic nerve activity suggest that hyperventilation alone does not necessarily increase sympathetic outflow or HR[9], and that these effects may depend on concurrent metabolic and chemical factors such as CO_2 levels.

Although these mechanisms are well understood, most previous studies have investigated slow breathing mainly through changes in frequency, with limited attempts to control MV independently. Respiratory interventions typically adjust RR while allowing TV to vary naturally, which makes it difficult to isolate the specific contributions of frequency and volume. It is therefore unclear whether the respiratory effect on cardiovascular and autonomic function is driven by respiratory frequency, MV, or the interaction between them. Our study separates the independent and interactive effects of RR and MV through a systematically controlled breathing protocol designed to assess their influence on cardiovascular and autonomic function.

Understanding the relative contributions of respiratory frequency and MV is critical for establishing respiratory modulation as an effective intervention. If MV plays a dominant role in cardiovascular modulation, then protocols that rely only on slowing respiratory frequency may not provide optimal cardiovascular and autonomic benefits. Conversely, if RR and MV exert distinct or synergistic effects on autonomic regulation, then multifactorial interventions targeting both parameters may be warranted. Moreover, ventilation-driven changes in CO may have broader physiological consequences, including potential effects on cerebrospinal fluid (CSF) circulation and on brain clearance mechanisms[8,10], which are increasingly recognized as important targets for intervention in neurological health and disease[11]. Therefore, the present study aimed to (1) quantify the independent effects of RR and MV on cardiovascular outcomes (HR, SV, and CO) and autonomic function (HRV) during controlled breathing, and (2) determine which of the two parameters exerts a greater and more consistent influence on these responses. We hypothesized that MV would serve as the global primary determinant across all evaluated parameters. Based on our findings, this hypothesis was only partially supported; while MV emerged as the dominant driver of systemic cardiovascular outcomes (specifically HR and CO), RR was found to be the primary factor modulating autonomic outcomes (specifically HRV).

Methods

Participants

Nineteen healthy young participants from the Republic of Korea were enrolled in this study (Table 1). All participants provided written informed consent prior to the experiment. The research team explained the study objectives and experimental procedures to all participants before the experiment began. Inclusion criteria required participants to have no known cardiovascular, respiratory, or neurological disorders. Exclusion criteria included a history of hypertension or cardiac arrhythmia, asthma or autonomic dysfunction, and anxiety-related or other psychiatric disorders. Current use of medications known to affect cardiovascular or autonomic function (e.g., beta-blockers or anxiolytics) was also grounds for exclusion. To minimize acute confounds, participants were instructed to abstain from alcohol consumption and strenuous physical activity for 24 h prior to testing, to obtain at least 8 h of sleep the night before the experiment, and to refrain from caffeine intake on the day of testing.

Ethics approval

This study was approved by the Institutional Review Board of Hanyang University (IRB No. HYU-2024-037). All procedures were performed in accordance with the Declaration of Helsinki and relevant guidelines and regulations. Written informed consent was obtained from all participants before participation.

Experimental design

The experimental protocol consisted of three sequential phases: a 5-minute resting phase with spontaneous breathing to establish a baseline, a training phase in which participants practiced the assigned breathing condition until they could stably follow the target RR and respiratory volume, and a 5-minute experimental task phase during which participants performed the trained breathing pattern (Fig. 1a). Within each condition, participants wore the mouthpiece connected to the airflow sensor continuously across all three phases (Resting, Training, and Experimental Task phase), so that the baseline and the task were recorded under identical instrumented breathing.

Characteristics	Value
Total number of participants, n	19
Age, mean (SD)	24.6 (1.2)
Female gender, n (%)	16(84)
Male gender, n (%)	3(16)
Minute ventilation, mean (SD)	4.50 (1.73) L/min
Tidal volume, mean (SD)	392.2 (229.1) mL
Respiratory rate, mean (SD)	13.1 (3.4)

Table 1. Participant characteristics

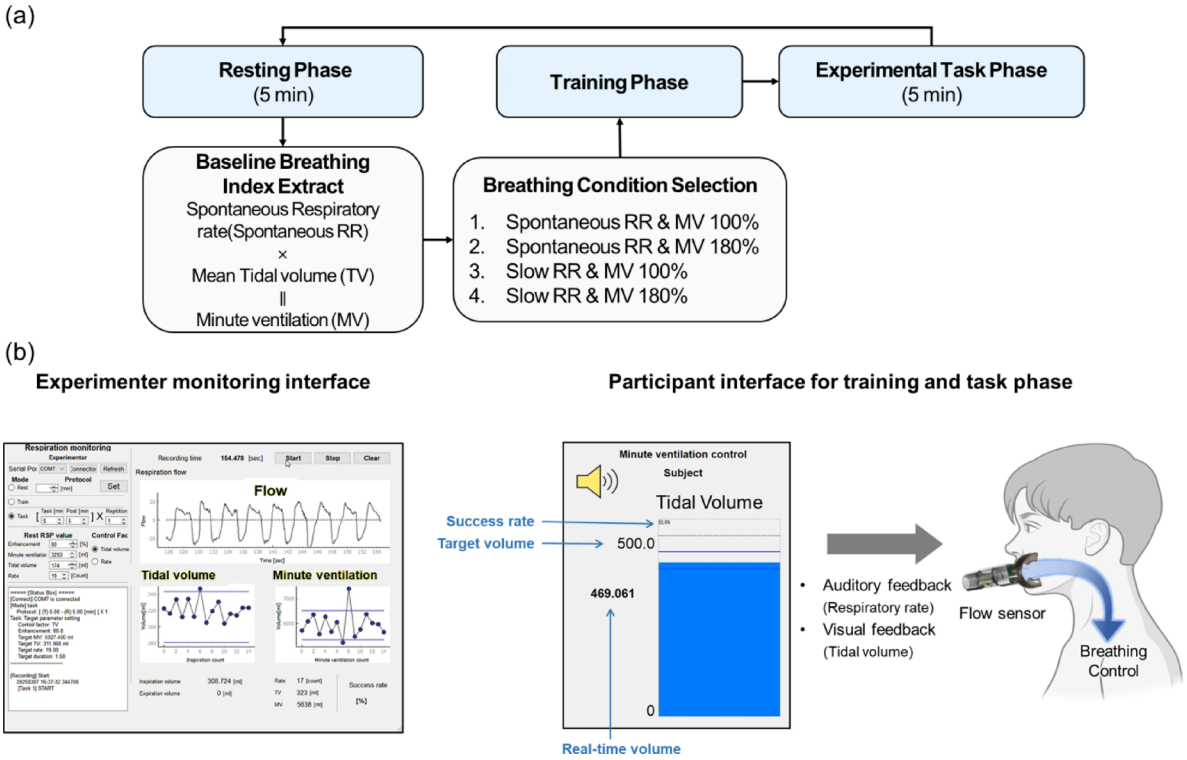

Fig. 1. Experimental protocol and breathing feedback system. (**a**) Schematic of the three-phase workflow (5-min rest to define baseline indices; training with real-time feedback; 5-min task). (**b**) Custom interface presenting breathing flow, RR, TV, and MV; auditory pacing tones guided RR and a visual bar guided TV. Training completion was defined as maintaining target TV within ± 10% for 10 consecutive breaths. A demonstration of the interface and training is available in Supplementary Video S1. The mouthpiece and airflow sensor were worn throughout all three phases of each condition and removed only during the inter-condition rest periods.

Each participant completed this full sequence under four different breathing conditions. The order of conditions was randomized independently for each participant to minimize systematic carryover, learning, and fatigue effects. To further prevent carryover effects between conditions, a minimum rest period of 10 min was provided after each session. The mouthpiece was removed during the rest periods separating successive conditions, allowing participants to recover with unconstrained breathing between conditions. Following the rest period, participants were verbally asked whether they required additional recovery time before proceeding to the next condition. The four conditions were:

1. Spontaneous Respiratory Rate (Spontaneous RR) with MV 100%.
2. Spontaneous RR with MV 180%.
3. Slow RR (6 breaths/min) with MV 100%.
4. Slow RR with MV 180%.

The 'Spontaneous RR' condition used each participant's average respiratory rate recorded during the resting phase. MV settings were defined relative to the average MV obtained in the resting phase, where MV 100% indicates TV adjusted to maintain the measured Rest MV, while MV 180% represents an 80% increase above the Rest MV. We confirmed during the training session that all participants could comfortably perform the MV 180% condition without difficulty before proceeding to the main experiment. The Slow RR was fixed at 6 breaths/min, consistent with widely used protocols for deep breathing[7,11].

To standardize the physiological respiratory demand across participants, MV was employed as the primary independent variable rather than TV. Given that baseline respiratory parameters (Spontaneous RR and TV) vary significantly between individuals, modulating TV to achieve a fixed percentage of resting MV (e.g., 100% or 180%) allowed for a consistent ventilatory load. For instance, in the Slow RR (6 breaths/min) condition at 180% MV, the required TV was dynamically adjusted for each participant to compensate for their specific resting baseline, ensuring that the relative ventilatory load was standardized based on each individual's baseline. This individualized adjustment is crucial because baseline Spontaneous RR varies across participants (e.g., ranging from 10 to 16 breaths/min). If a participant with a Spontaneous RR of 10 breaths/min targets the Slow RR (6 breaths/min) at 180% MV, their TV must expand by a factor of $(10 / 6) \times 1.8 = 3$. Conversely, for a participant with a Spontaneous RR of 12 breaths/min, the required TV expansion factor becomes $(12 / 6) \times 1.8 = 3.6$. Because the required TV expansion ratio is fundamentally dependent on each individual's baseline RR, the predetermined

minute ventilation targets were experimentally achieved by individually tailoring the required TV on a subject-by-subject basis while controlling the respiratory rate. This protocol standardized the ventilatory load strictly in relative terms (i.e., 100% or 180% of each participant's individual resting minute ventilation), recognizing that absolute values were not necessarily uniform across participants, rather than shifting TV by a fixed percentage.

The training and experimental task phases were controlled using guided auditory and visual feedback to control both the RR and TV. Participants were instructed to breathe according to the feedback, which was provided through a custom interface providing real-time RR, TV, MV, and a breathing flow waveform (Fig. 1b). Notably, the same feedback system remained active and was continuously provided throughout the task phase to ensure that participants maintained the target breathing pattern. Breathing-rate pacing was delivered through auditory tones following a seven-note scale, which ascended during inspiration (do–re–mi–fa–so–la–ti–do) and descended during expiration (do–ti–la–so–fa–mi–re–do) to guide respiratory timing. TV feedback was presented as a visual bar that increased in real time during inspiration to facilitate matching the target TV. Each condition was individually trained and performed, allowing systematic evaluation of cardiovascular and autonomic changes under controlled breathing patterns.

Training for each condition was considered complete when participants maintained the target TV within ± 10% for 10 consecutive breaths, after which the task phase commenced. Most participants achieved this criterion within approximately 5 min across all conditions. A live demonstration of the system and training workflow is provided in Supplementary Video S1.

Measurements and data acquisition

Continuous cardiovascular signals, including HR, SV, and CO, were recorded using a BIOPAC system (ECG100C, NICO100C) throughout all phases. ECG signals were acquired at a sampling frequency of 1,000 Hz using the BIOPAC ECG100C module. Electrodes were placed in a 3-lead configuration using medical-grade Ag/AgCl electrodes positioned on the upper and lower abdomen. SV was measured using the BIOPAC NICO100C module, which employs impedance cardiography (ICG) with a sampling frequency of 1,000 Hz. Electrodes were placed at the neck and thorax following a standard four-electrode configuration in accordance with the manufacturer's guidelines. ICG has been widely employed as a noninvasive tool for assessing cardiovascular responses in healthy subjects in respiratory and autonomic research settings[12]. HRV was quantified using the standard deviation of normal-to-normal intervals (SDNN) and root mean square of successive differences (RMSSD) index, which represents the time-domain standard deviation of sinus rhythm R–R intervals and reflects overall beat-to-beat variability and autonomic nervous system activity. Respiratory flow was continuously measured using the Sensirion SFM3300- AW proximal mass flow sensor (Sensirion AG, Stäfa, Switzerland), a medical-grade device designed for respiratory applications. The sensor provides bidirectional flow measurement over ± 250 slm with a typical accuracy of ± 3% of measured value and is factory-calibrated for air. The sensor was coupled to a custom mouthpiece assembly via a standard 22 mm medical cone connector and interfaced with an in-house Python-based software system (Fig. 1b) at an effective sampling rate of approximately 60 Hz. TV was computed by time-integration of the incoming flow signal, RR was derived by dividing 60 by the total duration of each inspiratory–expiratory cycle, and MV was calculated as the product of RR and TV. These parameters were displayed in real time on the monitoring interface and used for participant feedback and protocol control throughout the experiment. Prior to the experiment, measurement accuracy was verified by repeated injections of a known volume using a 100 mL calibrated syringe; the mean volumetric error was 1.85 ± 1.63%, which is within the manufacturer's specified accuracy range of ± 3% of measured value. Raw flow values were referenced to the sensor's factory calibrati on standard (20 °C, 1 atm, dry air); the acquisition software applied real-time correction for ambient temperature and water vapor pressure in accordance with the manufacturer's recommended procedure. Standard BTPS (Body temperature and pressure, Saturated) or STPD (Standard temperature and pressure, dry) correction was not applied. Because MV targets were defined as a percentage relative to each participant's resting baseline MV - measured under identical ambient conditions within the same session - the BTPS correction factor is consistent across Resting and Experimental Task phases and does not alter the relative MV ratio used for protocol control. Through this system, respiratory flow was measured continuously with this sensor connected to a mouthpiece, from which RR, TV, and MV were derived in real time. Within each breathing condition, participants breathed through this mouthpiece during all three phases (Resting, Training, and Experimental Task phase), so that respiratory and cardiovascular signals in the baseline and the task were acquired under identical instrumentation. The mouthpiece was removed only during the rest periods separating successive conditions. Nose clips were not used, and participants breathed through the mouthpiece with the nasal passage unobstructed during the Resting, Training, and Experimental Task phases. Prior to each experimental session, participants were instructed to breathe exclusively through the mouthpiece and to refrain from nasal breathing throughout all experimental phases. Compliance was continuously monitored by the experimenter through direct visual observation. The software utilized the sensor data to set target conditions and provide real-time visual and auditory feedback during the training and task phases.

Data analysis

HR was derived from ECG recordings using the following signal processing pipeline. R-peaks were detected by applying an 8–25 Hz bandpass filter, consistent with the Pan–Tompkins QRS detection framework[13], followed by peak detection with a fixed amplitude threshold and a minimum inter-peak interval of 333 ms (corresponding to a physiological upper limit of ≈ 180 bpm). Beat-to-beat R–R intervals (RR_i, in seconds) were computed from successive R-peaks, and instantaneous HR was obtained as $HR = 60 / RR_i$ (beats·min^{-1}), then averaged over each phase.

HRV was quantified from beat-to-beat R–R intervals using two time-domain metrics: SDNN, reflecting overall autonomic variability, and RMSSD, reflecting short-term vagal modulation[14]. Frequency-domain indices

were not computed because slow breathing at 6 breaths/min (0.1 Hz) shifts RSA into the LF band (0.04–0.15 Hz), confounding standard spectral interpretation[15]. Both metrics were averaged over each 5-minute phase and expressed as percentage change from the resting baseline.

SV was calculated using the Kubicek equation[16]:

$$SV = \rho \times (L/Zo)^2 \times T \times |dZ/dt|_{max}$$

where SV is stroke volume (mL); ρ is blood resistivity, assumed constant at 147 Ω·cm (a standard value); L is the distance between the voltage-sensing electrodes (cm); Z_0 is the basal thoracic impedance (Ω); LVET is the left ventricular ejection time (s); and $|dZ/dt|_{max}$ is the maximum rate of change of the thoracic impedance during systole ($\Omega \cdot s^{-1}$). LVET was determined on a beat-by-beat basis[17] as follows. The raw dZ/dt signal was bandpass-filtered (1–7 Hz, 4th-order Butterworth, applied with zero-phase filtfilt) to attenuate motion and respiratory noise while preserving the cardiac ejection waveform[18], and its first derivative was computed to identify the fiducial points[19,20]. The B-point (onset of aortic valve opening) was identified as the last negative-to-positive zero-crossing of this derivative within a ± 100–150 ms window centered on the ECG R-peak[19]. The T-wave end was taken as the minimum of the ECG signal in the 200–600 ms window after the R-peak. The X-point (aortic valve closure, corresponding to the dZ/dt nadir) was identified as the first negative-to-positive zero-crossing of the derivative in the window from 100 to 200 ms after the B-point to 100 ms beyond the T-wave end[20]. LVET was computed as the interval between the B-point and the X-point, and $|dZ/dt|_{max}$ was extracted as the peak value of the filtered dZ/dt within this interval.

CO was computed as the product of HR and SV, based on the physiological relationship that:

$$CO\,(mL/min) = HR\,(beats/min) \times SV\,(mL/beat)$$

To isolate the effects of RR and MV, we compared modulation conditions that differed either in RR or TV while keeping the other constant. By directly comparing paired conditions, we aimed to exclude redundant breathing tasks and focus on the specific cardiovascular effects attributable to changes in ventilation rate or volume.

For each condition, we calculated the average values of HR, SV, and CO during the 5-minute task phase and compared them to the 5-minute resting baseline. In addition, 1-minute segmented averages were analyzed to assess temporal dynamics during modulation period.

Percentage change for each cardiovascular parameter was calculated as

$$Percentage\ \ change = \frac{task\ phase - resting\ phase}{resting\ phase} \times 100$$

.

where $\overline{task\ phase}$ and $\overline{resting\ phase}$ denote the mean values during the Task and Resting phases, respectively.

Heart rate variability (HRV) was quantified in the time domain from successive normal-to-normal (NN) sinus rhythm R–R intervals over each 5-minute phase using two primary metrics: SDNN and RMSSD. SDNN estimates overall HR variability and is mathematically defined as the standard deviation of the NN intervals over the given recording period:

$$SDNN = \sqrt{\frac{1}{N-1}\sum_{i=1}^{N}\left(RR_i - \overline{RR}\right)^2}$$

where N denotes the total number of successive R-R intervals, RR_i represents the duration of the i-th R-R interval (in milliseconds), and $\overline{RR}$ denotes the mean duration of all R-R intervals during the 5-minute phase:

$$\overline{RR} = \frac{1}{N}\sum_{i=1}^{N} RR_i$$

RMSSD reflects short-term, beat-to-beat variations and serves as a surrogate index for cardiac parasympathetic (vagal) modulation. It is calculated as the root mean square of the differences between adjacent, successive R-R intervals:

$$RMSSD = \sqrt{\frac{1}{N-1}\sum_{i=1}^{N-1}(RR_{i+1} - RR_i)^2}$$

where $RR_{i+1} - RR_i$ represents the difference in duration between consecutive adjacent R-R intervals (in milliseconds), and N-1 denotes the total number of successive differences analyzed within the 5-minute epoch.

Crucially, all percentage changes in cardiovascular parameters (HR, SV, and CO) and autonomic metrics reported in this study were calculated relative to the initial, unconstrained 5-minute Resting phase (spontaneous breathing through the mouthpiece, without pacing feedback), which served as the true statistical baseline (0%). Because the mouthpiece and airflow sensor were in place during both the resting baseline and the task phase, any baseline-to-task change reflects the imposed breathing pattern (RR/MV) and the associated pacing demand rather than the presence of the breathing apparatus. The experimental task conditions, including the Spontaneous RR with MV 100% condition, were subsequently compared against this condition-specific resting baseline to evaluate the independent and interactive effects of RR and MV.

Statistical analysis

Data are presented as mean ± standard error of the mean (SEM). The normality of the data was assessed using the Shapiro-Wilk test. To evaluate the effects of the two respiratory factors, a two-way repeated-measures ANOVA was performed with RR (spontaneous vs. slow) and MV (100% vs. 180%) as within-subject factors. When significant main effects or interactions were observed, post hoc pairwise comparisons were conducted using Bonferroni's multiple comparisons test within GraphPad Prism. Crucially, all 95% confidence intervals (CIs) and adjusted p-values for specific condition differences reported in the Results were derived directly from these post hoc Bonferroni matrices calculated by Prism. Effect sizes were reported using partial eta-squared (η_p^2) for the main and interaction effects in the two-way RM ANOVA, and Cohen's d for the post-hoc paired comparisons. All heart rate variability (HRV) parameters, including percentage changes, estimates, and their corresponding 95% CIs, have been comprehensively re-verified against the original raw datasets to ensure total exactness and consistency throughout the manuscript.

Temporal changes across the 5-minute task phase were evaluated using repeated-measures one-way ANOVA on 1-minute segmented averages. For all ANOVA procedures, Mauchly's test was used to assess the assumption of sphericity; where this assumption was violated, degrees of freedom were corrected using the Greenhouse–Geisser epsilon. Effect sizes were reported using partial eta-squared (η_p^2) for ANOVA and Cohen's d for paired comparisons, along with 95% confidence intervals (CIs). Statistical significance was set at $p < 0.05$ (or the adjusted p-value for multiple comparisons).

To determine whether the physiological changes from the resting baseline to the task phase were significant within each breathing condition, two-tailed paired t-tests were performed.

Use of artificial intelligence tools

The authors used ChatGPT (OpenAI) solely for English language editing to improve readability.

Results

Cardiovascular responses to minute ventilation and respiratory rate modulation

Percentage changes in HR, SV, and CO across the four breathing modulation conditions are shown in Fig. 2. A two-way RM ANOVA revealed a significant main effect of MV on HR ($F(1, 18) = 40.33$, $p < 0.0001$, $\eta_p^2 = 0.29$). Post-hoc pairwise comparisons using Bonferroni's multiple comparisons test generated the adjusted p-values and 95% confidence intervals (CIs) for specific condition differences. When MV increased to 180% while maintaining the Spontaneous RR, HR increased significantly by 7.78% (95% CI: 3.75–11.81%; $p_{bonf} = 0.0001$). Similarly, under the Slow RR condition, increasing MV to 180% resulted in a significant HR elevation of 5.11% (95% CI: 1.49–8.73%; $p_{bonf} = 0.0034$).

In contrast, SV showed no statistically significant main effects or interactions (all $p > 0.05$). Specifically, when MV increased to 180%, no significant changes in SV were observed under either Spontaneous RR (-4.42%; 95% CI: -11.86 to 3.02%; $p_{bonf} = 0.5733$) or Slow RR (-1.89%; 95% CI: -11.04 to 7.26%; $p_{bonf} > 0.9999$).

For CO, there was a significant main effect of MV ($F(1, 18) = 10.39$, $p = 0.0047$, $\eta_p^2 = 0.17$) and a significant interaction between RR and MV ($F(1, 18) = 8.23$, $p = 0.0102$). Under Spontaneous RR, increasing MV to 180% led to a significant CO increase of 12.42% (95% CI: 3.39–21.45%; $p_{bonf} = 0.0043$). However, under Slow RR, the CO change was not statistically significant (6.18%; 95% CI: -3.06 to 15.42%; $p_{bonf} = 0.3784$).

To assess the independent effect of RR, we compared Spontaneous RR versus Slow RR while maintaining constant MV. At MV 100%, reducing RR from rest to 6 breaths/min resulted in no significant changes in HR (3.57%; 95% CI: -1.75 to 8.89%; $p_{bonf} = 0.3730$), SV (-0.74%; 95% CI: -8.15 to 6.67%; $p_{bonf} > 0.9999$), or CO (3.23%; 95% CI: -1.19 to 7.64%; $p_{bonf} = 0.2638$). Similarly, at MV 180%, no significant changes were observed between RR conditions for HR (-0.90%; 95% CI: -3.09 to 4.89%; $p_{bonf} > 0.9999$), SV (3.27%; 95% CI: -2.47 to 9.01%; $p_{bonf} = 0.6518$), or CO (3.01%; 95% CI: -2.73 to 8.76%; $p_{bonf} = 0.8245$).

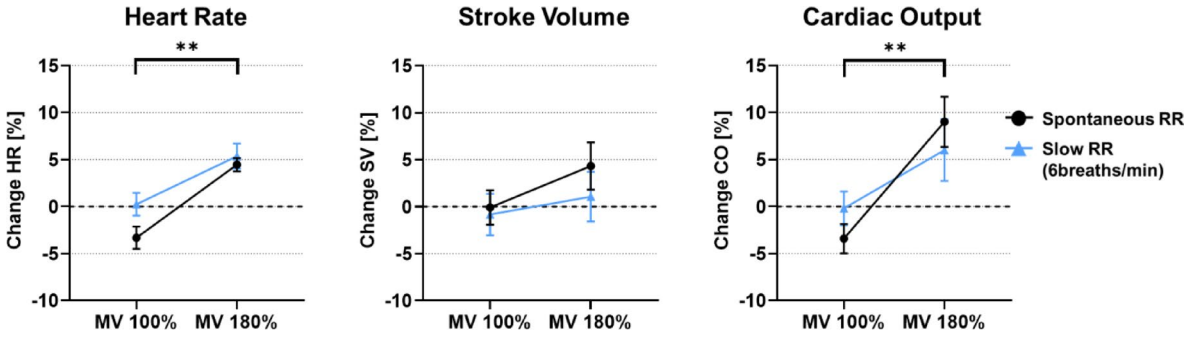

Fig. 2. Percentage changes in heart rate, stroke volume, and cardiac output across four breathing modulation conditions. Mean ± SEM percentage change relative to resting baseline during four breathing conditions ($n = 19$). Black circles represent Spontaneous RR conditions, and blue triangles represent Slow RR (6 breaths/min) conditions. Within each respiratory rate group, conditions differ in minute ventilation (100% vs. 180%). Asterisks indicate significant main effects of time as determined by repeated measures two-way ANOVA main effect of MV (*$p < 0.05$, **$p < 0.001$).

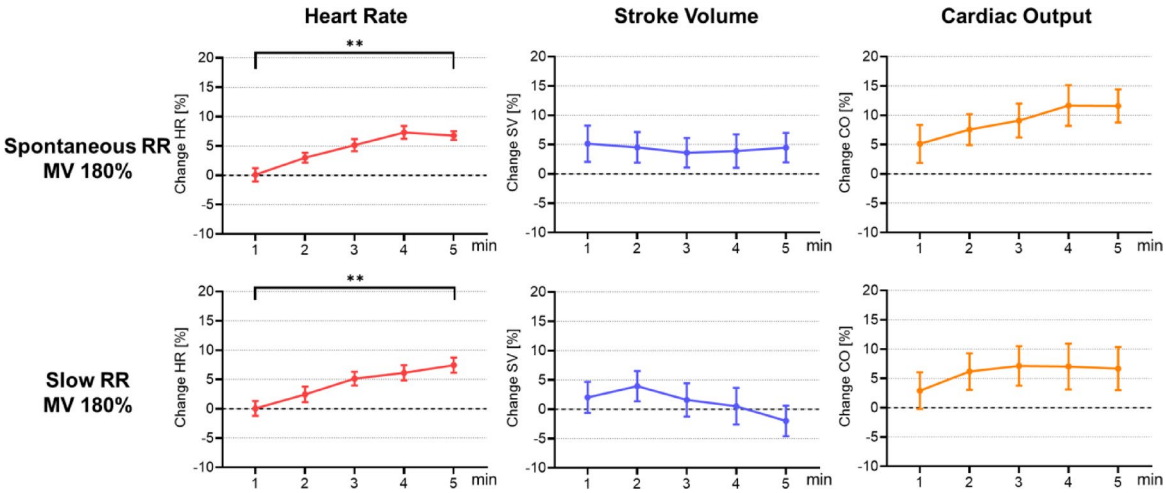

Fig. 3. Temporal changes in heart rate, stroke volume, and cardiac output during task phase under elevated minute ventilation conditions. One-minute averages (mean ± SEM) of HR (left), SV (middle), and CO (right) during the 5-minute task phase at MV 180% for Spontaneous RR (top row, red lines) and Slow RR (6 breaths/min; bottom row, blue lines) conditions ($n = 19$). Lines show temporal evolution across each minute of the task period relative to baseline. Asterisks indicate significant main effects of time as determined by repeated measures one-way ANOVA (*$p < 0.05$, **$p < 0.005$) within each condition.

Variable	Effect	Degrees of freedom (DFn, DFd)	F-statistic	*P* value
	MV main effect	1.000,18.00	40.33	$P < 0.001$
HR	RR main effect	1.000,18.00	2.665	$P = 0.1199$
	MV x RR interaction	1.000,18.00	2.767	$P = 0.1135$
	MV main effect	1.000,18.00	1.639	$P = 0.2167$
SV	RR main effect	1.000,18.00	1.279	$P = 0.2729$
	MV x RR interaction	1.000,18.00	0.8626	$P = 0.3653$
	MV main effect	1.000,18.00	10.39	$P = 0.0047$
CO	RR main effect	1.000,18.00	0.006192	$P = 0.9382$
	MV x RR interaction	1.000,18.00	8.231	$P = 0.0102$

Table 2. Two-way repeated-measures ANOVA results for the effects of RR and MV

The temporal dynamics of cardiovascular responses during the breathing task under high MV are illustrated in Fig. 3, which presents changes in HR, SV, and CO under MV 180% conditions (Table 2).

HR exhibited a robust and progressive increase throughout the modulation period under both RR conditions. Under Spontaneous RR, HR increased significantly over time ($F(1.81, 32.61) = 15.49$, $p < 0.0001$, $\eta_p^2 = 0.46$), with a significant elevation observed between the first and fifth minutes (Mean diff = 6.67%, 95% CI: 2.73–10.62%; $p_{bonf} = 0.0007$). Similarly, under Slow RR, HR rose gradually ($F(2.43, 43.77) = 22.64$, $p < 0.0001$, $\eta_p^2 = 0.56$), showing a substantial increase by the fifth minute compared to the first minute (Mean diff = 7.38%, 95% CI: 4.40–10.37%; $p_{bonf} < 0.0001$).

In contrast, SV displayed differing temporal patterns depending on the RR condition. Under Slow RR, SV showed a significant time-dependent change ($F(2.01, 36.08) = 5.12$, $p = 0.0110$, $\eta_p^2 = 0.22$). While it appeared to decline from the 2-minute peak toward the 5-minute mark, the specific comparison between the first and fifth minutes did not reach statistical significance after Bonferroni correction (Mean diff = 4.01%, 95% CI: -1.15 to 9.17%; $p_{bonf} = 0.1795$). Under Spontaneous RR, SV remained stable throughout the task with no significant temporal changes ($F(1.82, 32.71) = 0.25$, $p = 0.7558$, $\eta_p^2 = 0.01$).

Consequently, CO stabilization showed different primary drivers over time. Although CO showed an upward trend, the temporal effect did not reach statistical significance under either Spontaneous RR ($F(1.94, 34.94) = 3.04$, $p = 0.0619$, $\eta_p^2 = 0.14$) or Slow RR ($F(2.16, 38.88) = 2.17$, $p = 0.1247$, $\eta_p^2 = 0.11$). Specifically, the difference between the 1-minute and 5-minute time points was not significant for either condition (Spontaneous RR: $p_{bonf} = 0.1956$; Slow RR: $p_{bonf} = 0.5562$).

These data suggest that while CO elevation is maintained throughout the task, the progressive rise in HR serves as the more consistent driver of this response compared to SV, particularly as the task persists. The temporal dynamics under MV 100% conditions are shown in Supplementary Fig. S1.

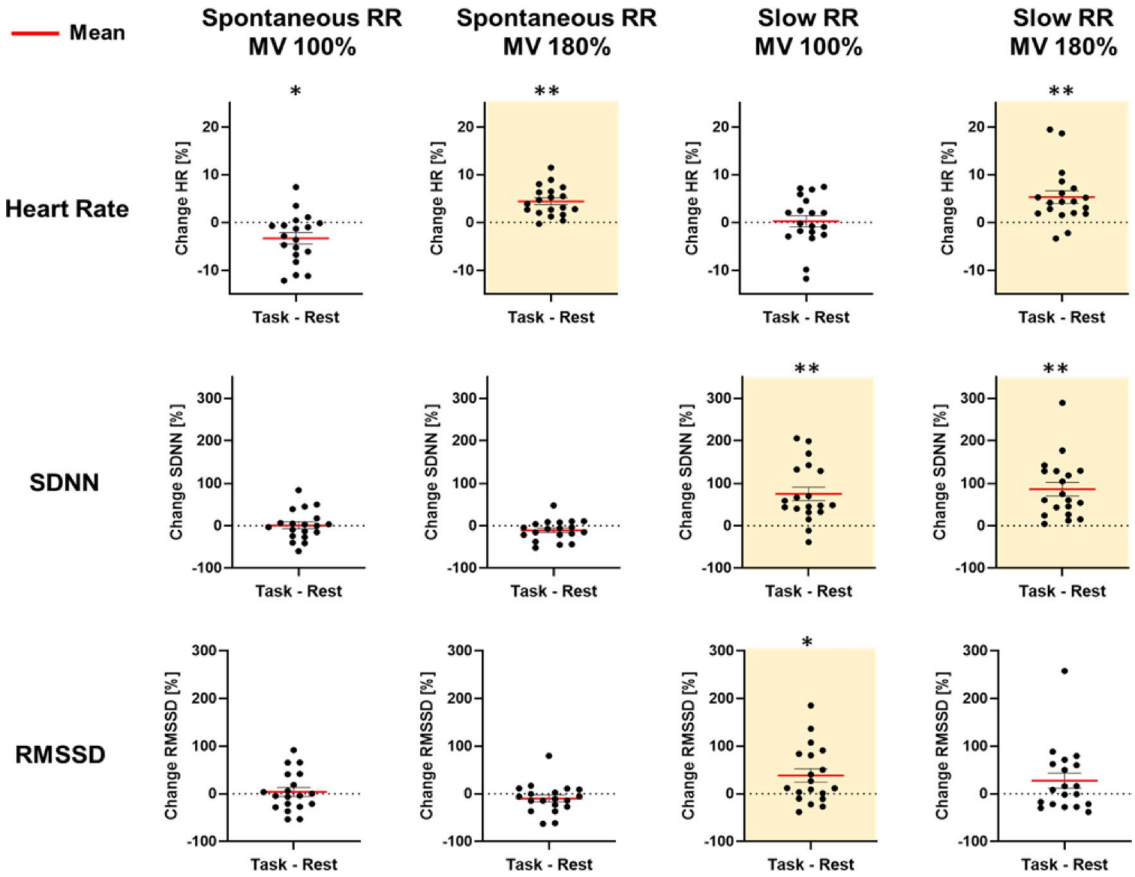

Fig. 4. Individual changes in heart rate and heart rate variability across breathing modulation conditions. Individual data points (dots) and group mean ± SEM (horizontal line) for HR (left column) and heart rate variability (SDNN, RMSSD) during task phase relative to resting baseline ($n = 19$). Each panel represents one of four breathing conditions: Spontaneous RR with MV 100% (top left), Spontaneous RR with MV 180% (top right), Slow RR (6 breaths/min) with MV 100% (bottom left), and Slow RR with MV 180% (bottom right). Dotted lines indicate baseline. Statistical significance for the comparison between the task phase and resting baseline was determined using two-tailed paired t-tests, $\alpha = 0.05$; $^{*}p < 0.05$, $^{**}p < 0.01$

Autonomic responses: heart rate variability modulation across breathing conditions

The averaged changes in HR and HRV (SDNN) across the four breathing conditions are summarized in Fig. 4. Slow RR (6 breaths/min) produced robust increases in HRV regardless of minute ventilation: at MV 100%, SDNN increased by 75.08% (95% CI: 41.97–108.2%; Cohen's d = 1.09, $p < 0.01$), and at MV 180%, SDNN increased by 86.24% (95% CI: 52.08–120.4%; Cohen's d = 1.22, $p < 0.01$). To further evaluate parasympathetic modulation, RSSD was analyzed. Consistent with the SDNN results, Slow RR at MV 100% significantly increased RMSSD by 38.55% (95% CI: 9.26–67.84%; Cohen's d = 0.63, $p = 0.013$), indicating enhanced vagal tone. However, at MV 180%, the increase in RMSSD (27.58%) did ot reach statistical significance (95% CI: -5.94 to 61.11%; Cohen's d = 0.40, $p = 0.101$), suggesting that high MV may partially attenuate the parasympathetic enhancement typically seen with slow breathing.

In contrast, breathing at the Spontaneous RR did not significantly alter HRV. At MV 100%, neither SDNN (+0.87%) (95% CI: -16.04 to 17.79%; Cohen's d = 0.02, $p = 0.332$) nor RMSSD (+4.195%) (95% CI: -15.50 to 23.89%; Cohen's d = 0.10, $p = 0.660$) showed statistically significant changes. Similarly, at MV 180%, no significant changes were observed for SDNN (-10.82%) (95% CI: -22.41 to 0.77%; Cohen's d = 0.45, $p = 0.795$) or RMSSD (-970%) (95% CI: -24.82 to 5.41%; Cohen's d = 0.31, $p = 0.194$).

The condition Slow RR with MV 180% produced concurrent increases in both HR (4.45%) (95% CI: 2.54–8.17%; Cohen's d = 0.92, $p < 0.01$) and SDNN 8624% (95% CI: 52.08–120.4%; Cohen's d = 1.22, $p < 0.01$), while the ncrease in RMSSD (27.58%) remained a non-significant trend (95% CI: -5.94 to 61.11%; Cohen's d = 0.40, $p = 0.101$).

Discussion

This study systematically investigated how RR and MV independently and interactively influence cardiovascular and autonomic responses in healthy adults. By systematically varying RR and TV, we dissociated the respective contributions of breathing frequency and MV to changes in HR, SV, CO, and HRV. The results indicate that

increased MV elevates CO through a mechanism driven mainly by HR, whereas slow breathing produces distinct autonomic effects characterized by enhanced HRV.

Minute ventilation as the primary driver of cardiovascular modulation

Our findings show that MV, rather than breathing frequency alone, is the primary driver of acute hemodynamic responses in controlled breathing interventions. Specifically, increasing MV to 180% consistently elevated HR and CO regardless of respiratory rate, whereas changing RR alone (from rest to 6 breaths/min) at constant MV produced no significant cardiovascular effects. This observation challenges the conventional emphasis on breathing frequency in meditation and biofeedback protocols, suggesting MV as a key parameter in optimizing cardiovascular outcomes[6,21].

The mechanism underlying MV-driven cardiovascular modulation likely involves changes in intrathoracic pressure and venous return[22]. Increases in TV augment negative intrathoracic pressure during inspiration, enhancing venous return and cardiac preload, which can elevate SV and CO. In addition, large TV may stimulate pulmonary stretch receptors and mechanoreceptors, triggering reflexive adjustments in sympathetic and parasympathetic outflow[23]. Our observation that HR increased more consistently than SV under high-MV conditions suggests that autonomic adjustments, particularly sympathetic activation or vagal withdrawal, play a dominant role in mediating the cardiovascular response to elevated MV.

Temporal dynamics and the mechanistically biphasic cardiac output response

Within-task time-course analysis further revealed that this hemodynamic response unfolded in a mechanistically distinct phase. During the initial phase of modulation (minutes 1–2), HR remained relatively stable while SV increased substantially, consistent with the Frank-Starling-mediated preload augmentation driven by enhanced inspiratory venous return[24,25]. As high MV was sustained into the later phase (minutes 3–4), SV declined or plateaued while HR increased progressively, such that the continued elevation in CO was sustained predominantly through chronotropic mechanisms[26]. This temporal transition in the primary determinant of CO, from preload-mediated SV augmentation in the early phase to chronotropically driven elevation in the later phase, underscores the multi-phasic nature of cardiovascular adaptation to sustained ventilatory loading[27].

This pattern highlights the dynamic interplay between HR and SV in response to ventilation-driven hemodynamic stress and demonstrates the predominance of HR-mediated CO control under prolonged high-MV breathing conditions. This phenomenon aligns with classical cardiorespiratory physiology, where acute increases in ventilation, particularly through increases in TV, modulate intrathoracic pressure and venous return, thereby influencing preload and HR-mediated CO responses[28].

These temporal dynamics have important implications for designing respiratory interventions. Brief period of high-MV breathing may transiently enhance both SV and HR, which could be useful for acute cardiovascular challenges or warm-up protocols. In contrast, sustained high-MV breathing relies predominantly on HR-mediated CO control, which may have different metabolic and autonomic consequences. Understanding these temporal patterns can inform the development of tailored breathing protocols for clinical rehabilitation[29], and stress management[11].

Distinct HRV and cardiovascular patterns: potential concomitant autonomic influences

The HRV findings provide additional insight into autonomic regulation. Slow RR with resting MV significantly increased SDNN, and RMSSD - a time-domain index more specifically reflecting parasympathetic activity[14,30]- also showed an increasing trend under slow RR conditions, collectively consistent with enhanced vagal modulation during slow breathing[31,32]. In contrast, MV at 180% during resting RR produced a marked increase in HR without a corresponding HRV indices, consistent with heightened sympathetic activity or vagal withdrawal under conditions of elevated ventilatory demand[33].

Notably, the condition combining Slow RR with high MV (Slow RR + MV 180%) resulted in concurrent increases in both HR and SDNN.

Furthermore, the increasing trend in RMSSD observed under slow RR conditions persisted in this combined condition, providing preliminary parasympathetic specific evidence alongside the HR elevation[14]. This pattern departs from the typical inverse HR-HRV relationship, where increased HR is generally associated with reduced HRV due to sympathetic dominance and vagal withdrawal[34] However, an increase in HR combined with an elevation in SDNN does not directly demonstrate simultaneous sympathetic and parasympathetic co-activation. Notably, RMSSD, a surrogate marker more closely tied to pure vagal cardiac modulation, did not significantly increase in the slow RR plus high MV condition. Because our study did not include direct measurements of sympathetic nerve activity, catecholamines, baroreflex sensitivity, or frequency-domain parameters, this observational pattern should be interpreted cautiously as a phenomenon potentially compatible with concurrent, complex autonomic influences, serving as a hypothesis that requires direct verification in futurestudies. Future studies incorporating multimodal autonomic assessment are needed to determine whether this pattern represents true autonomic co-activation to elucidate its underlying mechanisms.

hysiological and potential translational implications

It is important to note that the cardiovascular changes observed in this study, while statistically significant, were relatively modest in magnitude (approximately 2–3%) and were derived from a small cohort of healthy young adults ($n = 19$). Therefore, the direct clinical translation of these findings should be approached with caution. Nevertheless, our results suggest potential implications for cardiorespiratory rehabilitation and ventilator management.

Previous studies have primarily focused on slow breathing and its benefits for vagal tone and HRV enhancement[35,36], with limited attention to the independent effects of MV. The present findings broaden this

perspective by demonstrating that increases in MV driven by TV, even when RR is held constant, meaningfully alter CO. This indicates that modulation of MV functions as a strong autonomic and hemodynamic stimulus, distinct from the effects of reduced respiratory frequency. Our results are consistent with emerging evidence that ventilation mechanics, including TV, inspiratory/expiratory ratio, and respiratory effort, play critical roles in cardiovascular regulation beyond simple respiratory frequency[37]. For example, studies using inspiratory muscle training have shown that increased inspiratory effort can enhance sympathetic activity and blood pressure responses, even without changes in RR[38].

Limitations and future directions

Several limitations should be acknowledged.

First, The study involved healthy young adults, limiting generalizability to older populations or patients with cardiopulmonary dysfunction. Age-related changes in cardiovascular compliance, autonomic function, and respiratory mechanics may alter responses to MV modulation. Future studies should include diverse age groups and clinical populations to assess the broader applicability of these findings.

Second, limitation is the absence of end-tidal CO_2 ($ETCO_2$) monitoring. Elevating MV to 180% likely induced a degree of hypocapnia, which may independently affect HR and HRV[35,36]. Although no participants reported hypocapnia-related symptoms such as dizziness or paraesthesia, future studies should incorporate real-time $ETCO_2$ monitoring to more precisely disentangle mechanical ventilatory effects from CO_2-mediated cardiovascular responses.

Third, Although we confirmed that all participants were healthy young adults without known cardiovascular or respiratory diseases, specific anthropometric data such as height, weight, and body mass index (BMI) were not recorded. These factors, along with individual physical activity levels and prior experience with breathing exercises, can influence resting cardiovascular parameters and respiratory mechanics. While the within-subject design of this study, where each participant served as their own control, helps to mitigate the confounding effects of these individual differences, the lack of detailed anthropometric profiling remains a limitation that may restrict the generalizability of our findings to a broader or more diverse population.

Fourth, the short-duration breathing tasks may not capture long-term adaptations to ventilation-driven modulation. Longitudinal intervention studies are needed to determine whether repeated exposure to high-MV breathing induces sustained changes in cardiovascular function, autonomic balance, or baroreflex sensitivity. Furthermore, although both cardiac output and respiratory-related pressure oscillations are known to contribute to CSF movement[39–41], we did not directly measure CSF flow, glymphatic function, or any neuroimaging outcomes in the present study. Therefore, any potential implications of our protocol on neurofluid circulation remain purely speculative and hypothesis-generating. Future studies incorporating direct neuroimaging modalities (e.g., real-time magnetic resonance imaging) are warranted to verify whether tailored therapeutic breathing interventions can practically support central neurofluid transport or glymphatic waste clearance.

Fifth, nose clips were not used during the experiment. Although participants were explicitly instructed to breathe exclusively through the mouthpiece and compliance was visually monitored throughout, the absence of nose clips means that minor nasal airflow cannot be entirely excluded, which may have introduced a small degree of measurement error in flow-derived respiratory parameters. This potentially explains why the baseline resting MV and TV appeared slightly low, leading to a minor underestimation of absolute values. However, this minor error would apply systematically across all conditions and is unlikely to affect the overall relative trends.

Sixth, a notable limitation of this study is the relatively small sample size ($n = 19$). As this was an exploratory study aimed at investigating the immediate cardiovascular responses to varied respiratory modulations, a formal power analysis was not performed a priori. Given the non-invasive and low-burden nature of the experimental protocol, we acknowledge that a larger cohort was feasible and would have provided greater statistical power to detect smaller effect sizes and support more definitive conclusions across the 2×2 factorial design. While the within-subject design partially mitigates this limitation by reducing inter-individual variability, our findings should be interpreted with caution. Future studies with larger cohorts, ideally enrolling at least 40–50 participants, are warranted to confirm these results and ensure broader generalizability of the physiological dynamics observed.

Seventh, HRV was assessed using time-domain metrics (SDNN and RMSSD) rather than frequency-domain indices. As the slow breathing condition at 6 breaths/min shifts RSA into the LF band (0.04–0.15 Hz), standard frequency-domain interpretation of sympathetic modulation (LF) and vagal activity (HF) is not valid under these conditions. Although time-domain metrics are less susceptible to this respiratory-driven spectral confound, they do not permit spectral decomposition of sympathetic and parasympathetic contributions, which constrains the mechanistic specificity of our autonomic inferences.

Eighth, SV was estimated using ICG, which is susceptible to respiratory artifacts. Large tidal volumes, as employed in the MV 180% conditions, may alter baseline thoracic impedance (Z_0) through changes in intrathoracic air content, potentially affecting SV estimates via the Z_0^2 term in the Kubicek equation. Although dZ/dt_max was extracted beat-by-beat within the ECG-referenced LVET window to limit temporal contamination by respiratory-frequency components, systematic modulation of Z_0 by large-TV breathing cannot be fully excluded. This limitation is inherent to ICG-based measurement under controlled breathing protocols and should be considered when interpreting the magnitude of SV and CO responses, particularly under high-MV conditions.

Finally, because no nose clip was used, minor nasal airflow may have modestly underestimated TV and MV—including the resting reference—across the Resting, Training, and Experimental Task phases; since this bias acts in the same direction in all phases, its effect on the within-condition percentage changes is expected to be largely offset. This limitation concerns only the ventilatory variables, as HR, SV, and CO were measured independently by ECG and ICG.

Conclusion

In summary, our study demonstrates that cardiorespiratory outcomes are distinctively partitioned: MV rather than RR alone emerges as the key determinant of short-term systemic CO modulation, whereas RR operates as the primary driver of overall heart rate variability (HRV) regardless of ventilatory volume. Consequently, our original hypothesis was only partially supported. These results highlight the necessity of distinguishing cardiovascular from autonomic findings when designing targeted respiratory protocols. In conclusion, while high minute ventilation drives the primary systemic cardiovascular responses, slow respiratory rate independently shapes heart rate variability. The combined state of slow breathing and elevated volume yields a unique physiological profile that is potentially compatible with concurrent autonomic influences, though direct confirmation of autonomic branch interactions remains a subject for subsequent research. These results support the development of targeted breathing protocols for autonomic regulation and cardio-neurovascular health and highlight the importance of considering minute ventilation alongside respiratory frequency in respiratory intervention strategies.

Data availability

The datasets generated and analyzed during the current study are available from the corresponding author upon reasonable request.

Received: 25 March 2026; Accepted: 29 June 2026
Published online: 15 July 2026

References

1. Bernardi, L. et al. Effect of rosary prayer and yoga mantras on autonomic cardiovascular rhythms: comparative study. *Bmj* **323**, 1446–1449 (2001).
2. Lehrer, P. et al. Heart rate variability biofeedback improves emotional and physical health and performance: A systematic review and meta analysis. *Appl. Psychophysiol. Biofeedback*. **45**, 109–129 (2020).
3. Pal, G. K. & Velkumary, S. Effect of short-term practice of breathing exercises on autonomic functions in normal human volunteers. *Indian J. Med. Res.* **120**, 115 (2004).
4. Bernardi, L., Porta, C. & Sleight, P. Cardiovascular, cerebrovascular, and respiratory changes induced by different types of music in musicians and non-musicians: the importance of silence. *Heart* **92**, 445–452 (2006).
5. Yasuma, F. & Hayano, J. Respiratory sinus arrhythmia: why does the heartbeat synchronize with respiratory rhythm? *Chest* **125**, 683–690. https://doi.org/10.1378/chest.125.2.683 (2004).
6. Benchetrit, G. Breathing pattern in humans: diversity and individuality. *Respir Physiol.* **122**, 123–129. https://doi.org/10.1016/s0034-5687(00)00154-7 (2000).
7. Seals, D. R. & Chase, P. B. Influence of physical training on heart rate variability and baroreflex circulatory control. *J Appl Physiol ()* 66, 1886–1895 (1989).) 66, 1886–1895 (1989). (1985). https://doi.org/10.1152/jappl.1989.66.4.1886
8. Liu, P. et al. Cardiac and respiratory activities induce temporal changes in cerebral blood volume, balanced by a mirror CSF volume displacement in the spinal canal. *Neuroimage* **305**, 120988. https://doi.org/10.1016/j.neuroimage.2024.120988 (2025).
9. St. Croix, C. M., Satoh, M., Morgan, B. J., Skatrud, J. B. & Dempsey, J. A. Role of respiratory motor output in within-breath modulation of muscle sympathetic nerve activity in humans. *Circul. Res.* **85**, 457–469 (1999).
10. Yatsushiro, S. et al. Characterization of Cardiac- and Respiratory-driven Cerebrospinal Fluid Motions Using a Correlation Mapping Technique Based on Asynchronous Two-dimensional Phase Contrast MR Imaging. *Magn. Reson. Med. Sci.* **20**, 385–395. https://doi.org/10.2463/mrms.mp.2020-0085 (2021).
11. Lehrer, P. M., Vaschillo, E. & Vaschillo, B. Resonant frequency biofeedback training to increase cardiac variability: rationale and manual for training. *Appl. Psychophysiol. Biofeedback*. **25**, 177–191. https://doi.org/10.1023/a:1009554825745 (2000).
12. Raaijmakers, E., Faes, T. J., Scholten, R. J., Goovaerts, H. G. & Heethaar, R. M. A meta-analysis of three decades of validating thoracic impedance cardiography. *Crit. Care Med.* **27**, 1203–1213 (1999).
13. Pan, J. & Tompkins, W. J. A real-time QRS detection algorithm. *IEEE Trans. biomedical engineering*, 230–236 (2007).
14. Shaffer, F. & Ginsberg, J. P. An Overview of Heart Rate Variability Metrics and Norms. *Front. Public. Health*. **5**, 258. https://doi.org/10.3389/fpubh.2017.00258 (2017).
15. Bernardi, L. et al. Effect of breathing rate on oxygen saturation and exercise performance in chronic heart failure. *Lancet* **351**, 1308–1311 (1998).
16. Systems, B. I. O. P. A. C. I. Application Note 215: Cardiac Output Measurement—Using NICO100C. (2007).
17. Lee, Q. Y. et al. Estimation of cardiac output and systemic vascular resistance using a multivariate regression model with features selected from the finger photoplethysmogram and routine cardiovascular measurements. *Biomed. Eng. Online*. **12**, 19 (2013).
18. Nagel, J. H. et al. New signal processing techniques for improved precision of noninvasive impedance cardiography. *Ann. Biomed. Eng.* **17**, 517–534. https://doi.org/10.1007/bf02368071 (1989).
19. Árbol, J. R. et al. Mathematical detection of aortic valve opening (B point) in impedance cardiography: A comparison of three popular algorithms. *Psychophysiology* **54**, 350–357 (2017).
20. Karpiel, I., Richter-Laskowska, M., Feige, D., Gacek, A. & Sobotnicki, A. An effective method of detecting characteristic points of impedance cardiogram verified in the clinical pilot study. *Sensors* **22**, 9872 (2022).
21. Meuret, A. E., Wilhelm, F. H. & Roth, W. T. Respiratory biofeedback-assisted therapy in panic disorder. *Behav. Modif.* **25**, 584–605. https://doi.org/10.1177/0145445501254006 (2001).
22. Mesquida, J., Kim, H. K. & Pinsky, M. R. Effect of tidal volume, intrathoracic pressure, and cardiac contractility on variations in pulse pressure, stroke volume, and intrathoracic blood volume. *Intensive Care Med.* **37**, 1672–1679. https://doi.org/10.1007/s00134-011-2304-3 (2011).
23. Richardson, C. A., Herbert, D. A. & Mitchell, R. A. Modulation of pulmonary stretch receptors and airway resistance by parasympathetic efferents. *J. Appl. Physiol. Respir Environ. Exerc. Physiol.* **57**, 1842–1849. https://doi.org/10.1152/jappl.1984.57.6.1842 (1984).
24. Skytioti, M., Søvik, S. & Elstad, M. Respiratory pump maintains cardiac stroke volume during hypovolemia in young, healthy volunteers. *J. Appl. Physiol.* **124**, 1319–1325 (2018).
25. Convertino, V. A. Mechanisms of inspiration that modulate cardiovascular control: the other side of breathing. *J. Appl. Physiol.* **127**, 1187–1196 (2019).
26. Fritzsche, R. G., Switzer, T. W., Hodgkinson, B. J. & Coyle, E. F. Stroke volume decline during prolonged exercise is influenced by the increase in heart rate. *J. Appl. Physiol.* **86**, 799–805 (1999).
27. Coyle, E. F. & Gonzalez-Alonso, J. Cardiovascular drift during prolonged exercise: new perspectives. *Exerc. Sport Sci. Rev.* **29**, 88–92 (2001).

28. Toska, K. & Eriksen, M. Respiration-synchronous fluctuations in stroke volume, heart rate and arterial pressure in humans. *J. Physiol.* **472**, 501–512. https://doi.org/10.1113/jphysiol.1993.sp019958 (1993).
29. Jang, M. H., Shin, M. J. & Shin, Y. B. Pulmonary and Physical Rehabilitation in Critically Ill Patients. *Acute Crit. Care*. **34**, 1–13. https://doi.org/10.4266/acc.2019.00444 (2019).
30. Laborde, S. et al. Effects of voluntary slow breathing on heart rate and heart rate variability: A systematic review and a meta-analysis. *Neurosci. Biobehavioral Reviews*. **138**, 104711 (2022).
31. Magnon, V., Dutheil, F. & Vallet, G. T. Benefits from one session of deep and slow breathing on vagal tone and anxiety in young and older adults. *Sci. Rep.* **11**, 19267 (2021).
32. Zaccaro, A. et al. How breath-control can change your life: a systematic review on psycho-physiological correlates of slow breathing. *Front. Hum. Neurosci.* **12**, 409421 (2018).
33. Pinna, G. D., Maestri, R., Rovere, L., Gobbi, M. T., Fanfulla, F. & E. & Effect of paced breathing on ventilatory and cardiovascular variability parameters during short-term investigations of autonomic function. *Am. J. Physiol-Heart C.* **290**, H424–H433 (2006).
34. Kazmi, S. Z. H. et al. Inverse correlation between heart rate variability and heart rate demonstrated by linear and nonlinear analysis. *PloS one*. **11**, e0157557 (2016).
35. Berg, T. & Jensen, J. Simultaneous parasympathetic and sympathetic activation reveals altered autonomic control of heart rate, vascular tension, and epinephrine release in anesthetized hypertensive rats. *Front. Neurol.* **2**, 71. https://doi.org/10.3389/fneur.2011.00071 (2011).
36. Eickholt, C. et al. Sympathetic and Parasympathetic Coactivation Induces Perturbed Heart Rate Dynamics in Patients with Paroxysmal Atrial Fibrillation. *Med. Sci. Monit.* **24**, 2164–2172. https://doi.org/10.12659/msm.905209 (2018).
37. Ramos-Barrera, G. E., DeLucia, C. M. & Bailey, E. F. Inspiratory muscle strength training lowers blood pressure and sympathetic activity in older adults with OSA: a randomized controlled pilot trial. *J. Appl. Physiol. (1985)*. **129**, 449–458. https://doi.org/10.1152/japplphysiol.00024.2020 (2020).
38. da Silva, R. B., Neves, V. R., Montarroyos, U. R., Silveira, M. S. & Sobral Filho, D. C. Heart rate variability as a predictor of mechanical ventilation weaning outcomes. *Heart Lung*. **59**, 33–36. https://doi.org/10.1016/j.hrtlng.2023.01.007 (2023).
39. Lim, S. et al. Human cerebrospinal fluid net flow enhanced by respiration during the awake state. *Nat. Commun.* **16**, 11499. https://doi.org/10.1038/s41467-025-66548-4 (2025).
40. Iliff, J. J. et al. A paravascular pathway facilitates CSF flow through the brain parenchyma and the clearance of interstitial solutes, including amyloid beta. *Sci. Transl Med.* **4**, 147ra111. https://doi.org/10.1126/scitranslmed.3003748 (2012).
41. Mestre, H. et al. Flow of cerebrospinal fluid is driven by arterial pulsations and is reduced in hypertension. *Nat. Commun.* **9**, 4878. https://doi.org/10.1038/s41467-018-07318-3 (2018).

Acknowledgements

This work was supported by the National Research Foundation of Korea (NRF) grant funded by the Korea government (MSIT) (No. RS-2023-00266075). This work was supported by the Technology Innovation Program (RS-2025-13302968) funded By the Ministry of Trade, Industry & Resources (MOTIR, Korea).

Author contributions

H. Choi designed the study, performed the experiments, analyzed the data, and wrote the manuscript.C. Kim developed the breathing feedback system software and assisted with data acquisition and analysis.J. Lee, S. Lim and P. H. Min contributed to data interpretation and discussion of results throughout the study.D.P. Jang supervised and directed the project.All authors reviewed and approved the final manuscript.

Funding

This work was supported by the National Research Foundation of Korea (NRF) grant funded by the Korea government (MSIT) (No. RS-2023-00266075). This work was supported by the Technology Innovation Program (RS-2024-00445152, Development of cardiovascular disease prediction/analysis/monitoring meta patch and continuous measurement wearable product for biosignals) funded By the Ministry of Trade, Industry & Resources (MOTIR, Korea).

Competing interests

Dong Pyo Jang is the founder and CEO of Hypertix, and holds shares in the company. The remaining authors declare no competing interests.

Additional information

Supplementary Information The online version contains supplementary material available at https://doi.org/10.1038/s41598-026-60600-z.

Correspondence and requests for materials should be addressed to D.P.J.

Reprints and permissions information is available at www.nature.com/reprints.

Publisher's note Springer Nature remains neutral with regard to jurisdictional claims in published maps and institutional affiliations.

Open Access This article is licensed under a Creative Commons Attribution-NonCommercial-NoDerivatives 4.0 International License, which permits any non-commercial use, sharing, distribution and reproduction in any medium or format, as long as you give appropriate credit to the original author(s) and the source, provide a link to the Creative Commons licence, and indicate if you modified the licensed material. You do not have permission under this licence to share adapted material derived from this article or parts of it. The images or other third party material in this article are included in the article's Creative Commons licence, unless indicated otherwise in a credit line to the material. If material is not included in the article's Creative Commons licence and your intended use is not permitted by statutory regulation or exceeds the permitted use, you will need to obtain permission directly from the copyright holder. To view a copy of this licence, visit http://creativecommons.org/licenses/by-nc-nd/4.0/.

© The Author(s) 2026